FEBS Letters 585 (2011) 1054–1060

journal homepage: www.FEBSLetters.org

Label-free optical biosensor with microfluidics for sensing ligand-directed functional selectivity on trafficking of thrombin receptor

Vasiliy Goral, Qi Wu, Haiyan Sun, Ye Fang *

Biochemical Technologies, Science and Technology Division, Corning Inc., Corning, NY 14831, United States

ARTICLE INFO

Article history:
Received 22 December 2010
Revised 13 February 2011
Accepted 1 March 2011
Available online 4 March 2011

Edited by Christian Griesinger

Keywords:
Dynamic mass redistribution
G protein-coupled receptor
Ligand-directed functional selectivity
Microfluidics
Optical biosensor
Protease activated receptor-1

ABSTRACT

Ligand-directed functional selectivity has stimulated much interest in the molecular delineation of drug pharmacology and the process of drug discovery. Here we describe the development of a label-free optical biosensor with microfluidics for whole cell sensing. The microfluidics controls the duration of agonist exposure and of the functional recovery of activated protease activated receptor-1 (PAR_1). The biosensor manifests that the persistency of PAR_1 signaling is dependent on the agonists, which, in turn, affects the receptor resensitization process. This study demonstrates a new means to differentiate ligand-directed functional selectivity on trafficking of receptors.

1. Introduction

Ligand-directed functional selectivity or biased agonism is originated from the observations that many G protein-coupled receptor (GPCR) ligands exhibit different abilities to produce certain but not all receptor behaviours [1–3]. This is illustrated by different proteases that elicit distinct responses through the activation of protease activated receptor-1 (PAR_1, thrombin receptor) [4]. Thrombin is the main coagulation protease that can proteolytically activate PAR_1, resulting in pro-inflammatory responses and disruption of endothelial barrier [5]. Activated protein C, also an anti-coagulant protease, binds to its co-factor endothelial protein C receptor, which, in turn, cleaves and activates PAR_1, leading to anti-inflammatory responses and stabilization of endothelial barrier [6]. Synthetic peptide agonists (PAR activating peptides, PAR-APs) including SFLLR that mimic the N-terminus tethered ligand domain can activate PAR_1 independently of proteolysis [7]. The PAR-AP agonists were found to favour $G_{\alpha q}$ activation over $G_{\alpha 12/13}$, opposite to thrombin, in a human endothelial cell line [8]. The pathway selective activities of PAR_1 agonists add new revenue in elucidating PAR_1 signaling and functions in various tissues and cell types. However, biased agonism of PAR_1, in general GPCR ligands, is mostly measured via various signaling molecules [9]; and in most cases the signaling and cell type-specific responses elicited by different PAR_1 agonists remain poorly understood [4].

Resonant waveguide grating (RWG) biosensor is a nano-grating waveguide-based optical biosensor [10] that has attracted much interest in the molecular delineation of receptor biology and ligand pharmacology [11–14], because it enables non-invasive, sensitive and integrative measures of cell signaling based on stimulus-induced dynamic mass redistribution (DMR) in living cells [15–17]. However, in typical biosensor cellular assays a ligand is introduced using a pipetting system and cells are continuously exposed to the ligand, thus creating a static and sustained stimulation scheme [10]. Such an assay format may mask certain biased activities of various ligands. To overcome this, we here describe the development of a microfluidic RWG biosensor system and its uses for detecting ligand-directed functional selectivity on trafficking of PAR_1.

2. Materials and methods

2.1. Materials

Thrombin and cycloheximide were obtained from Sigma Chemical Co. (St. Louis, MO, USA). Argatroban was obtained from Tocris

Abbreviations: DMR, dynamic mass redistribution; GPCR, G protein-coupled receptor; PAR_1, protease activated receptor-1; PAR-AP, PAR activating peptide; RWG, Resonant waveguide grating biosensor

* Corresponding author. Fax: +1 607 974 5957.
E-mail address: fangy2@corning.com (Y. Fang).

0014-5793/$36.00
doi:10.1016/j.febslet.2011.03.003

Chemical Co. (St. Louis). SFLLR-amide was obtained from Bachem (King of Prussia, PA, USA). Epic® 384-well biosensor microplates and inserts were obtained from Corning Inc. (Corning, NY, USA). Poly-dimethylsiloxane (PDMS) was obtained from Dow Chemical (Midland, MI, USA). Live/Dead staining kits and sulforhodamine B were from Invitrogen (Carlsbad, CA, USA).

2.2. Cell culture

Human lung adenocarcinoma epithelial cell line A549 was obtained from American Type Cell Culture. The cells were cultured in the cell culture medium (Dulbecco's modified Eagle's medium (DMEM) supplemented with 10% fetal bovine serum (FBS) and 100 μg/ml penicillin and streptomycin) at 37 °C under air/5% CO_2.

2.3. Fabrication of microfluidic biosensor devices

Soft lithography was used to fabricate the microfluidic device using PDMS (poly-dimethylsiloxane) replicas [18]. Briefly, features on chrome mask were transferred onto silicon wafers using standard photolithographic process. The photoresist-defined silicon wafers were then anisotropically etched to a desired depth in a multiplex inductively coupled plasma etching system (Surface Technology Systems, Newport, NJ, USA). After photoresist removal and coating using trichloro(1*H*,1*H*,2*H*,2*H*-perfluorooctyl)silane, a PDMS pre-polymer solution containing a mixture of PDMS oligomers and a reticular agent (10:1 mass ratio) (Sylgard 184® Kit, Dow Corning Corp., Midland, MI, USA) was cast onto the etched silicon wafers and cured at room temperature for about 24 h to minimize shrinkage after curing. Next, the PDMS replicas were carefully peeled away from the wafers. Finally, after punching inlet and outlet holes, the PDMS replica was aligned and reversibly bonded onto the top of Epic® biosensor inserts.

For cell culture, the device, tubing (Tygon S-54-HL, Saint-Gobain Performance Plastics, Akron, OH, USA) and syringes (500 μl, gas tight 1700 series, Hamilton, Reno, NV, USA) were first sanitized with 70% ethanol. The microfluidic chambers were then filled with the cell culture medium. After cell seeding and sequential 4 h incubation, tubings were plugged into the microchamber inlets and were connected to syringes that were connected to a syringe pump (Model: SP230IW; World Precision Instruments, Sarasota, FL, USA). Afterwards, the cells were cultured overnight at 37 °C under air/5% CO_2 and perfusion of the cell culture medium at a flow rate of 5 μl/h.

2.4. DMR assays under static and sustained stimulation condition using Epic® system

Epic® system (Corning Inc.) is a wavelength interrogation reader system tailored for RWG biosensors in microtiter plates [10,11]. The detector uses integrated fiber optics to record the kinetics of cellular responses with a time interval of ~15 s. Twenty thousand cells per well were directly seeded and cultured overnight before assays. After washed twice, the cells were maintained with the assay vehicle (HBSS; 1× Hanks' balanced salt solution, 20 mM Hepes, pH 7.1) and further incubated inside the system for 1 h. Afterwards, a 2-min baseline was first established. Compound solutions were then transferred using the onboard liquid handler, and the cellular responses were recorded. Here compounds remained in the wells once added, and the cells were exposed to the compound(s) throughout the assays, thus creating a static and persistent stimulation condition. Further, since cells are sensitive to environmental changes, it would be difficult to completely replace the compound solution using conventional pipetting.

2.5. DMR assays under perfusion conditions using a RWG imager system

We recently developed a whole microplate RWG biosensor imager system [19]. For DMR assays under perfusion conditions, the imager was modified to increase spatial solution as well as to accommodate the reduced footprint of the microfluidic biosensor device. Specifically, a tunable light source is passed through a polarizer to generate a polarized light, which is then expanded through optical lens and mirrors to simultaneously illuminate at a normal incident angle all biosensors within the microfluidic device. The tunable light source linearly scans the wavelength range from 826 to 838 nm in every 3 s, such that the biosensor array is illuminated and synchronously imaged by a 1400 × 1024 pixel complementary metal oxide semiconductor camera (Dalsa Inc., Ontario, Canada). The spectral images are processed online to extract the resonant wavelengths. In order to minimize assay variability as well as the impact of time lag across the biosensor, cells only located within the central area of a biosensor (0.2 × 2 mm) were sampled to generate an averaged response.

2.6. Quantitative real-time PCR

Total RNA was extracted from A549 cells using RNeasy mini kit (Qiagen, Cat#74104). To eliminate genomic DNA contamination, on-column DNase digestion was performed using RNase-free DNase set (Qiagen, Cat#79254). The concentration and quality of total RNA were determined using Nanodrop 8000 (Thermo Scientific). Customized PCR-array plates for 352 GPCR genes and reagents were ordered from SABiosciences. About 1 μg total RNA was used for each 96-well PCR-array. The PCR-array was performed on an ABI 7300 Real-Time PCR System following manufacturer instructions.

2.7. Fluorescence microscopy

Live/Dear cell staining was carried out using the protocol recommended by the supplier. A Zeiss Axioplan fluorescence microscope was used to collect all fluorescence and light images.

3. Results

3.1. Prototyping microfluidic biosensor system

We first developed a prototype of microfluidic RWG biosensor system (Fig. 1). The microfluidic device consists of a 4 × 8 array of biosensors, each biosensor having a dimension of 2 mm × 2 mm and the array having a footprint that is compatible to a standard 384-well microplate. The device also contains a 4 × 4 array of microfluidic chambers, each having three inlets and one outlet, and the microchamber array covering a 4 × 8 array of biosensors so only one biosensor is centered in each microchamber and its adjacent biosensor is sacrificed. Syringe pumps are connected to the inlets to deliver solutions at a controlled flow rate. The distance from an inlet to the outlet is 9 mm, the central width of the chamber 5 mm, and the height of the microchannel 200 μm. The total volume required to fill up a chamber is 6 μl. To minimize the impact of shear force on cell biology, a flow rate of 1–5 μl/min was used. Given the microfluidic configurations we estimated that the shear force is $<2.5 \times 10^{-2}$ dyn/cm^2, well below those commonly used to trigger activation of certain signaling cascades such as extracellular signal-regulated kinases and N-terminal Jun kinase in certain cells [20,21].

To monitor cellular responses, we also developed a RWG imager that is capable of simultaneously imaging all biosensors within an

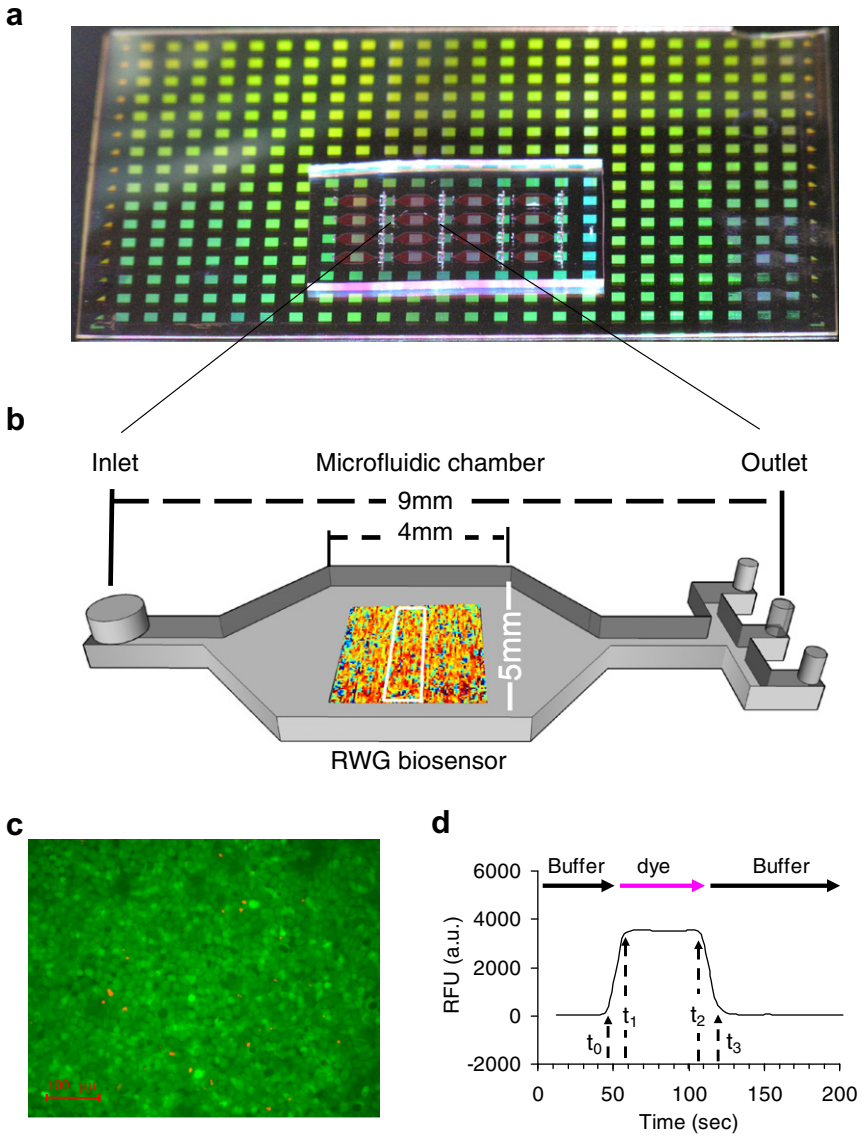

Fig. 1. A microfluidic RWG biosensor array for whole cell sensing. (a) A false coloured image of the biosensor array recorded using a digital camera by titling the biosensor plate under white light until a resonance condition was achieved. Different colours were seen due to difference in environment surrounding each sensor. Biosensors within the microfluidic device were pre-filled with the cell medium solution. (b) Schematic of a microfluidic chamber (open view). The false coloured image is an actual resonant image of a biosensor obtained using the RWG imager. The biosensors were covered with a monolayer of A549 cells via overnight culture. The white box indicates the location at which the cellular responses were monitored. (c) Fluorescence image of cells on the biosensor in (b) after Live/Dead staining. The green fluorescence indicates cells alive, and the red died cells. (d) The fluorescence intensity of the sampled area as a function of time. Here a 2 μl fluorescent dye solution (10 μg/ml sulforhodamine B) was perfused between the two perfusion steps with the assay buffer. The flow rate for all three steps was the same (2 μg/min).

array. This imager has a spatial resolution of 25 μm and a temporal resolution of 3 s. Fig. 1b showed a resonant wavelength image of a biosensor, wherein the biosensor was covered with a monolayer of A549 cells (Fig. 1c). Cell viability testing using the Live/Dead staining protocol suggests that almost all cells were viable.

To characterize the microfluidics device, a microchamber having no cells was sequentially perfused with the assay buffer, a fluorescent dye solution (10 μg/ml sulforhodamine B) for 1 min, and the assay buffer again, all at a constant flow rate of 2 μl/min. This created a 2 mm wide dye solution sandwiched between the two buffer solutions. The kinetics of the dye solution passing through the device was examined using fluorescence microscopy. The fluorescence intensity at the sampled area, as indicated by the white box (0.2 × 2 mm) in Fig. 1b, was recorded 1 min after the dye injection (Fig. 1d). Results showed that at t_0 (49 s) the fluorescence intensity started rising, indicating that the dye molecules reached the area. At t_1 (57 s) the fluorescence intensity reached the maximum, suggesting that the rising time to reach the injected concentration is <8 s. At t_2 (110 s) the fluorescence intensity started decaying, suggesting that the second buffer started to deplete the dye solution in the sampled area. At t_3 (118 s) the fluorescence intensity was back to the baseline, suggesting that the rinsing time to completely deplete the fluorescent molecules at the sampled area is <8 s. Narrowing down the sampled area can further improve the accuracy of measurements. Nonetheless, these results suggest that the microfluidic system is effective to control the duration of agonist stimulation and receptor recovery.

3.2. mRNA expression of PARs in A549

Quantitative real time PCR was used to examine expression of PARs in A549. Results showed that A549 expresses mRNA of

PAR_1, PAR_2 and PAR_3, whose threshold cycle (C_t) value was found to be 22, 22, and 24, respectively. No mRNA was detected for PAR_4. The C_t values were 21 and 15 for two control genes, hypoxanthine phosphoribosyltransferase 1 and β-actin, respectively.

3.3. DMR characteristics of PAR_1 activation

Both thrombin and SFLLR were used to activate the PAR_1 under both static and perfusion conditions. Results showed that under both conditions SFLLR resulted in a dose dependent DMR signal, which shares almost identical DMR characteristics (Fig. 2a) and EC_{50} value (4.1 ± 0.4 μM, $n = 3$ and 3.9 ± 0.6 μM, $n = 3$ for static and perfusion conditions, respectively). Similar results were obtained for thrombin, whose EC_{50} values were identical (0.60 ± 0.14 unit/ml) under both conditions (Fig. 2b and c). Perfusion with 10 unit/ml thrombin in the presence of 10 μM argatroban, a thrombin inhibitor, significantly suppressed the thrombin signal (Fig. 2d). The thrombin DMR in the presence of argatroban did not contain any immediate rapid rising phase, suggesting that the bulk index effect is minimal. Further, perfusion with lipid-free and protease-free bovine serum at a high concentration (0.025 wt.%) triggered a quite small response largely due to its bulk index, suggesting that any signal from non-specific absorption of proteins (e.g., thrombin and serum), if at all, is minimal. Together, these results suggest that A549 expresses functional PAR_1 and the perfusion had little effect on PAR_1 agonist induced DMR signals.

3.4. Desensitization and resensitization of PAR_1 signaling under distinct stimulation conditions

Homologous desensitization is a hallmark of GPCR signaling. Thus, the cross-desensitization between thrombin and SFLLR was first examined under the static and sustained stimulation condition using a previously developed DMR desensitization assay [22]. Results showed that under the static stimulation condition both SFLLR (10 μM) and thrombin (10 unit/ml), each at a saturating dose, resulted in a similar positive-DMR that is sustained for at least 2 h. Further, the 2nd stimulation with SFLLR only slightly altered the 1st thrombin-induced DMR, and the same was observed for thrombin in the SFLLR-treated cells (Fig. 3a), suggesting that thrombin and SFLLR cross-desensitized each other. Similar results were observed when the two perfusion steps between the first and second agonists were performed sequentially (Fig. 3d). These results suggesting that both agonists activate the same receptor, PAR_1.

Next, we examined DMR patterns of A549 cells upon repeated stimulations with PAR_1 agonists when an additional perfusion with the assay vehicle was introduced between the first and second agonist perfusion. Here the cells were first perfused with the first agonist for 30 min, followed by a perfusion with the assay vehicle for a given period of time (i.e., recovery time), and then a perfusion with the second agonist (thrombin). In this way, the receptor resensitization was allowed by the control of recovery time via the continuous flow of the assay vehicle to deplete the first agonist after the

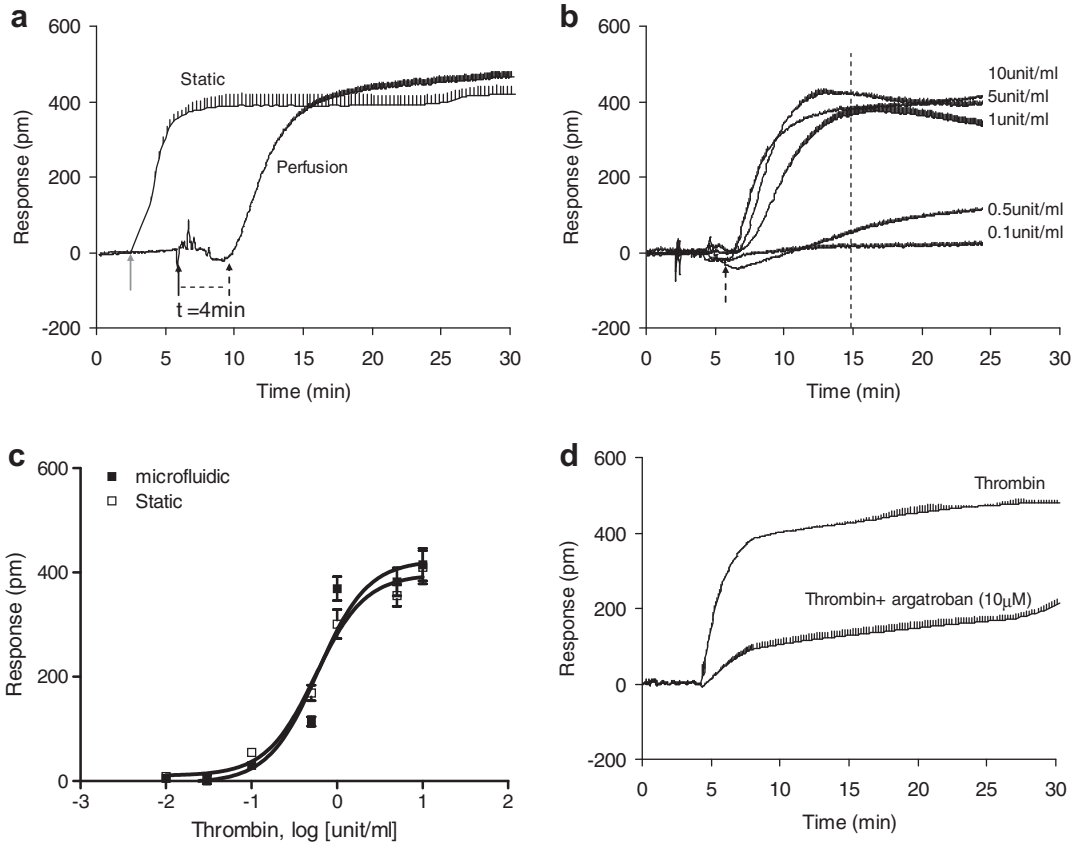

Fig. 2. DMR signals of PAR_1 agonists. (a) The DMR of A549 cells responding to SFLLR-amide (10 μM) obtained under the static and flow conditions. The grey arrow indicates the time SFLLR was added. The solid black arrow indicates the time when the perfusion starts, and the broken arrow the time when the agonist solution reaches the sampled area, between the two of which is a 4 min time lag. (b) The DMR of A549 responding to thrombin at different doses under the perfusion condition. The broken line indicates the DMR amplitudes used for EC_{50} calculation. (c) The amplitudes of the thrombin DMR as a function of thrombin doses. (d) The DMR of A549 cells responding to perfusion with thrombin (10 unit/ml) in the absence and the presence of 10 μM argatroban. All error bars represented the standard deviation of at least three replicates.

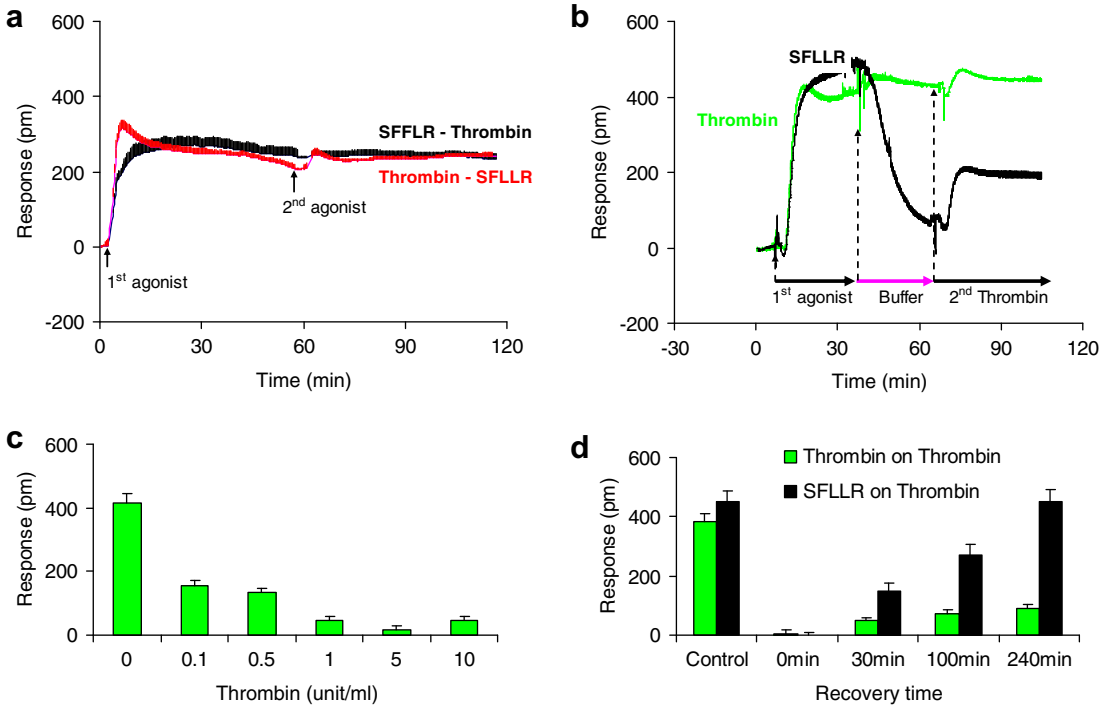

Fig. 3. Desensitization and resensitization of PAR_1 signaling in A549 cells. (a) SFLLR and thrombin cross-desensitized each other when the cells were repeatedly stimulated under the static and sustained condition. Here the DMR assays were carried out using Epic® system, wherein after the initial 2 min baseline recording, two agonist solutions (the 1st agonist and the 2nd agonist) were added into the same well having cultured cells in a sequential manner using conventional pipetting, and the two steps were separated about 1 h. The cellular responses were continuously monitored throughout the assays. (b) DMR signals of cells responding to repeated stimulations when an additional perfusion with the assay vehicle was introduced between the 1st (5 unit/ml thrombin, or 10 μM SFLLR) and 2nd agonist (10 unit/ml thrombin) stimulation. Each step was continuous for ~30 min. (c) The amplitudes of the 2nd thrombin induced DMR as a function of the doses of the 1st thrombin. The recovery time between the two stimulations was set to be 30 min. (d) The amplitudes of the 2nd thrombin induced DMR as a function of the recovery time. Thrombin was at 10 unit/ml thrombin, and SFLLR at 10 μM. The agonist responses of the assay vehicle-treated cells were used as positive controls. Similar protocol was used for obtaining (b–d). Briefly, the cell layer was sequentially perfused with (1) the assay buffer for 10 min to achieve a baseline, (2) the 1st agonist (thrombin or SFLLR) for 30 min to result in the first stimulation, (3) the assay buffer for a specific period of time to allow the functional recovery of the activated PAR_1, and (4) finally the 2nd agonist (thrombin) for 30 min to study the resensitization of the activated PAR_1. All error bars represented the standard deviation of at least three replicates.

receptor activation. The resensitization of A549 cells after the PAR_1 activation was measured based on the second thrombin induced DMR. Results showed that when the recovery time was set to be 30 min, removal of thrombin (5 unit/ml) caused the cells respond to the second thrombin stimulation with a small DMR signal (Fig. 3b). Conversely, removal of SFLLR (10 μM) caused the cells respond to the second thrombin with a significant DMR (Fig. 3b). Further, the higher concentration the first thrombin the smaller the second thrombin-induced DMR is (Fig. 3c). Lastly, the longer recovery time the greater response induced by the second thrombin is, and the recovery of functional PAR_1 was much faster in the SFLLR-activated cells than the thrombin-activated cells (Fig. 3d). These results suggest that PAR_1 resensitization is dependent on three factors: (1) types of PAR_1 agonists; (2) doses of PAR_1 agonists; and (3) the recovery time.

Interestingly, SFLLR or thrombin, each at a saturating dose, resulted in an elevated positive DMR that prolongs for at least 2 h when the cells were continuously exposed to the agonists under static or perfusion condition (Fig. 3a). However, the thrombin DMR was not altered by removal of thrombin 30 min after stimulation (Fig. 3b). Conversely, removal of SFLLR 30 min after stimulation rapidly reversed the course of its DMR back to a much lower level (Fig. 3b). This suggests that certain signaling pathways induced by SFLLR require persistent agonist occupancy.

Finally, we examined the mechanisms of PAR_1 resensitization. Here, cells were pre-exposed to cycloheximide for about 1 h, followed by stimulation with thrombin in the presence of cycloheximide for 30 min. Afterwards, the first thrombin was removed, and the cells were perfused with cycloheximide for 30 min. Finally, the cells were then stimulated again with the second PAR_1 agonist, SFLLR or thrombin. Cycloheximide is an inhibitor of protein biosynthesis via interfering with the translocation step in protein synthesis [23]. Results showed that the presence of cycloheximide altered the characteristics of the first thrombin induced DMR signals (Fig. 4 vs Figs. 2 and 3b). Further, when the recovery time was set to be 30 min and cycloheximide was present throughout the assay, the thrombin activated cells completely lost their responsiveness to the succeeding thrombin stimulation, but regained their responsiveness to SFLLR (Fig. 4). These results suggest that persistent PAR_1 signaling requires de novo synthesis and receptor cycling back to cell membrane.

4. Discussion

Elucidation of ligand-directed receptor trafficking and signal termination is important to understand biological functions of the PAR_1 and therapeutic potentials of PAR_1 ligands. Here, we described a microfluidic RWG biosensor system which enables label-free cellular assays under the control of the duration of agonist exposure and of the functional recovery of activated receptors. Endogenous PAR_1 in A549 was used as a model system. Quantitative RT-PCR showed that A549 cells express mRNAs of PAR_1, PAR_2 and PAR_3, but not PAR_4. Further, DMR assays revealed that the PAR_1 is functional – both thrombin and SFLLR resulted in robust DMR signals, and cross-desensitized each other under the persistent stimulation conditions.

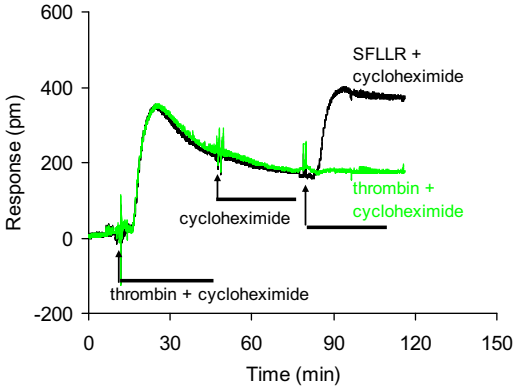

Fig. 4. The influence of cycloheximide on PAR_1 signaling in A549 cells. The cells were continuously exposed to cycloheximide of 10 μM throughout the assays. The doses for thrombin and SFLLR were 5 unit/ml, and 10 μM, respectively. All error bars represented the standard deviation of four replicates.

Thrombin and SFLLR were found to be different in regulating PAR_1 signaling. First, the functional recovery of activated PAR_1 induced by thrombin is much slower than that by SFLLR (Fig. 3d). This difference is attributed to the distinct abilities of the two agonists to cause receptor trafficking. Since SFLLR is known to cause receptor phosphorylation and internalization to an extent similar to thrombin [24,25], one possibility is that SFLLR has lower efficiency to result in the internalized receptors sorting into lysosomes for degradation, compared to thrombin. Lysosomal sorting is necessary to prevent persistent signaling by activated PAR_1 [26–28].

Second, the thrombin-activated cells completely lost their responsiveness to the succeeding stimulation with thrombin, but not SFLLR, when the cells were continuously exposed to cycloheximide and the recovery time was set to be 30 min. This is consistent with previous reports that in some cells a steady-state level of cleaved receptors was detected on the cell surface after prolonged stimulation with thrombin [29,30]. In such a state, cells were refractory to thrombin but responded to SFLLRN. Interestingly, the presence of cycloheximide altered the thrombin DMR signal. It is known that PAR_1 is cycled tonically between an intracellular pool and cell surface membrane [31,32]; thus, it is possible that the intracellular receptor pool become less in the absence of protein synthesis via blockage by cycloheximide, and the persistent activation of PAR_1 by thrombin can quickly deplete the intracellular pool, leading to alterations in the thrombin DMR.

Lastly, thrombin triggered an elevated DMR that prolongs for at least 2 h, which was largely insensitive to thrombin removal. However, the SFLLR DMR quickly reversed its course after SFLLR removal. Given the integrative nature and dependence on protein trafficking and redistribution of DMR measurements [15–17], the reversibility of the SFLLR DMR after agonist removal is a surprise finding. It is believed that 30 min after agonist activation many GPCR signaling events are completed, or have already propagated [33]. Although a recent study suggests that removal of agonists indeed caused dissociation of β-arrestin from the phosphorylated β_2-adrenergic receptor [34], there is no any reports suggesting that agonist removal can rapidly reverse cell signaling pathway(s) downstream receptor activation. The molecular mechanisms underneath are currently under investigation.

In summary, we have developed a microfluidic RWG biosensor system for whole cell sensing. Using PAR_1 as a model, we have shown that such a system allows the control of the duration of agonist exposure as well as of the functional recovery of activated receptors, such that ligand-directed receptor trafficking and signal termination between thrombin and SFLLR can be differentiated. Further deconvoluting the cellular mechanisms underneath the functional difference between thrombin and PAR-APs, such as the ability of PAR-APs to trigger receptor degradation and the role of PAR_3 in regulating PAR_1 signaling [35], would be beneficial to understanding the biology and therapeutic potential of PARs. The microfluidic RWG biosensor system offers a new dimension in sensing ligand-directed functional selectivity acting on GPCRs.

References

[1] Kenakin, T.P. (1995) Agonist-receptor efficacy. II. Agonist trafficking of receptor signals. Trends Pharmacol. Sci. 16, 232–238.
[2] Kenakin, T.P. and Miller, L.J. (2010) Seven transmembrane receptors as shapeshifting proteins: the impact of allosteric modulation and functional selectivity on new drug discovery. Pharmacol. Rev. 62, 265–304.
[3] Urban, J.D., Clarke, W.P., von Zastrow, M., Nichols, D.E., Kobilka, B., Weinstein, H., Javitch, J.A., Roth, B.L., Christopoulos, A., Sexton, P.M., Miller, K.J., Spedding, M. and Mailman, R.B. (2007) Functional selectivity and classical concepts of quantitative pharmacology. J. Pharmacol. Exp. Ther. 320, 1–13.
[4] Russo, A., Soh, U.J.K. and Trejo, J. (2009) Proteases display biased agonism at protease-activated receptors: location matters! Mol. Interv. 9, 87–96.
[5] Komarova, Y.A., Mehta, D. and Malik, A.B. (2007) Dual regulation of endothelial junctional permeability. Sci. STKE 412, re8.
[6] Feistritzer, C. and Riewald, M. (2005) Endothelial barrier protection by activated protein C through PAR1-dependent sphingosine 1–phosphate receptor-1 crossactivation. Blood 105, 3178–3184.
[7] Coughlin, S.R. (1999) How the protease thrombin talks to cells. Proc. Natl. Acad. Sci. USA 96, 11023–11027.
[8] McLaughlin, J.N., Shen, L., Holinstat, M., Brooks, J.D., DiBenedetto, E. and Hamm, H.E. (2005) Functional selectivity of G protein signaling by agonist peptides and thrombin for the protease-activated receptor-1. J. Biol. Chem. 280, 25048–25059.
[9] Galandrin, S., Oligny-Longpre, G. and Bouvier, M. (2007) The evasive nature of drug efficacy: implications for drug discovery. Trends Pharmacol. Sci. 8, 423–430.
[10] Fang, Y. (2007) Non-invasive optical biosensor for probing cell signaling. Sensors 7, 2316–2329.
[11] Fang, Y. (2006) Label-free cell-based assays with optical biosensors in drug discovery. Assays Drug Dev. Technol. 4, 583–595.
[12] Kenakin, T. (2009) Cellular assays as portals to seven-transmembrane receptor-based drug discovery. Nat. Rev. Drug Discov. 8, 617–626.
[13] Fang, Y., Frutos, A.G. and Verkleeren, R. (2008) Label-free cell assays for GPCR screening. Comb. Chem. H.T.S. 11, 357–369.
[14] Schröder, R., Janssen, N., Schmidt, J., Kebig, A., Merten, N., Hennen, S., Müller, A., Blättermann, S., Mohr-Andrä, M., Zahn, S., Wenzel, J., Smith, N.J., Gomeza, J., Drewke, C., Milligan, G., Mohr, K. and Kostenis, E. (2010) Deconvolution of complex G protein-coupled receptor signaling in live cells using dynamic mass redistribution measurements. Nat. Biotechnol. 28, 943–949.
[15] Fang, Y., Li, G. and Peng, J. (2005) Optical biosensor provides insights for bradykinin B2 receptor signaling in A431 cells. FEBS Lett. 579, 6365–6374.
[16] Fang, Y., Ferrie, A.M., Fontaine, N.H. and Yuen, P.K. (2005) Characteristics of dynamic mass redistribution of EGF receptor signaling in living cells measured with label free optical biosensors. Anal. Chem. 77, 5720–5725.
[17] Fang, Y., Ferrie, A.M., Fontaine, N.H., Mauro, J. and Balakrishnan, J. (2006) Resonant waveguide grating biosensor for living cell sensing. Biophys. J. 2006 (91), 1925–1940.
[18] McDonald, J.C. and Whitesides, G.M. (2002) Poly(dimethylsiloxane) as a material for fabricating microfluidic devices. Acc. Chem. Res. 35, 491–499.
[19] Ferrie, A.M., Wu, Q. and Fang, Y. (2010) Resonant waveguide grating imager for live cell sensing. Appl. Phys. Lett. 97, 223704.
[20] Jo, H., Sipos, K., Go, Y.M., Law, R., Rongm, J. and McDonald, J.M. (1997) Differential effect of shear stress on extracellular signal-regulated kinase and N-terminal jun kinase in endothelial cells. G_{i2}- and $G_{\beta/\gamma}$-dependent signaling pathways. J. Biol. Chem. 272, 1395–1401.
[21] Hahn, C., Orr, A.W., Sanders, J.M., Jhaveri, K.A. and Schwartz, M.A. (2009) The subendothelial extracellular matrix modulates JNK activation by flow. Circ. Res. 104, 995–1003.
[22] Fang, Y. and Ferrie, A.M. (2007) Optical biosensor differentiates signaling of endogenous PAR1 and PAR2 in A431 cells. BMC Cell Biol. 8, 24.
[23] Obrig, T.G., Culp, W.J., McKeehan, W.L. and Hardesty, B. (1971) The mechanism by which cycloheximide and related glutarimide antihiotics inhibit peptide synthesis on reticulocyte ribosomes. J. Biol. Chem. 246, 174–181.
[24] Shapiro, M.J., Weiss, E.J., Faruqi, T.R. and Coughlin, S.R. (2000) Protease-activated receptors 1 and 4 are shut off with distinct kinetics after activation by thrombin. J. Biol. Chem. 275, 25216–25221.
[25] Hoxie, J.A., Ahuja, M., Belmonte, E., Pizarro, S., Parton, R. and Brass, L.F. (1993) Internalization and recycling of activated thrombin receptors. J. Biol. Chem. 268, 13756–13763.
[26] Chen, C.H., Paing, M.M. and Trejo, J. (2004) Termination of protease-activated receptor-1 signaling by β-arrestins is independent of receptor phosphorylation. J. Biol. Chem. 2004 (279), 10020–10031.
[27] Paing, M.M., Stutts, A.B., Kohout, T.A., Lefkowitz, R.J. and Trejo, J. (2002) β-Arrestins regulate protease-activated receptor-1 desensitization but not internalization or down-regulation. J. Biol. Chem. 277, 1292–1300.

[28] Macfarlane, S.R., Seatter, M.J., Kanke, T., Hunter, G.D. and Plevin, R. (2001) Proteinase-activated receptors. Pharmacol. Rev. 53, 245–282.
[29] Ishii, K., Hein, L., Kobilka, B. and Coughlin, S.R. (1993) Kinetics of thrombin receptor cleavage on intact cells. Relation to signaling. J. Biol. Chem. 268, 9780–9786.
[30] Trejo, J., Connolly, A.J. and Coughlin, S.R. (1996) The cloned thrombin receptor is necessary and sufficient for activation of mitogen-activated protein kinase and mitogenesis in mouse lung fibroblasts. Loss of responses in fibroblasts from receptor knockout mice. J. Biol. Chem. 271, 21536–21541.
[31] Hein, L., Ishii, K., Coughlin, S.R. and Kobilka, B.K. (1994) Intracellular targeting and trafficking of thrombin receptors. A novel mechanism for resensitization of a G protein-coupled receptor. J. Biol. Chem. 269, 27719–27726.
[32] Paing, M.M., Johnson, C.A., Siderovski, D.P. and Trejo, J. (2006) Clathrin adaptor AP2 regulates thrombin receptor constitutive internalization and endothelial cell resensitization. Mol. Cell. Biol. 26, 3231–3242.
[33] Lohse, M.J., Nikolaev, V.O., Hein, P., Hoffmann, C., Vilardaga, J.-P. and Bünemann, M. (2008) Optical techniques to analyze real-time activation and signaling of G-protein-coupled receptors. Trends Pharmacol. Sci. 29, 159–165.
[34] Krasel, C., Bünemann, M., Lorenz, K. and Lohse, M.J. (2005) β-Arrestin binding to the β2-adrenergic receptor requires both receptor phosphorylation and receptor activation. J. Biol. Chem. 280, 9528–9535.
[35] McLaughlin, J.N., Patterson, M.M. and Malik, A.B. (2007) Protease-activated receptor-3 (PAR3) regulates PAR1 signaling by receptor dimerization. Proc. Natl. Acad. Sci. USA 104, 5662–5667.